Paper No. T6-1.5, pp. 1-5

15th INTERNATIONAL SYMPOSIUM on
POWER ELECTRONICS - Ee 2009
XV Međunarodni simpozijum Energetska elektronika – Ee 2009
NOVI SAD, REPUBLIC OF SERBIA, October 28th - 30th, 2009

THE INFLUENCE OF OVERVOLTAGES ON CABLE-ELECTRIC MOTOR INSULATION SUBJECTED TO STEP WAVEFORMS

Barbara Florkowska, Marek Florkowski*, Jakub Furgał,
Piotr Pająk, Józef Roehrich, Rafał Tarko, Paweł Zydroń
AGH University of Science and Technology,
Department of Electrical and Power Engineering, Kraków, Poland
*ABB Corporate Research, Kraków, Poland

Abstract: *Special problems in PWM (Pulse-width-modulated) supplied induction motors arise from overvoltages and partial discharges (PD) in insulating systems of cables and machines. The PWM wave form products complex overvoltages that stress the insulation to more severely than normal sinusoidal voltage waveforms. In-service stresses cause degradation of high voltage insulating systems. The overvoltages have a form of fast switching pulses with very short rise time, composed of repetitive sequences. Such conditions have essential influence on inception and activity of partial discharges and space charge accumulation in insulation of cable supplying the motor and the motor insulation. Some aspects of these problems are presented in the paper: the modeling of overvoltages at motor terminals, the influence of length of supplying cable, the influence of rise time of the PWM pulses, and the experimental results of overvoltages recorded at motor terminals with varied the supplying cable length and pulse rise times.*

The PD mechanism, as a result of the PWM pulses approximated by a trapezoidal wave with a varying rise time, is described and laboratory experiments are presented. The phase-resolved PD patterns were registered by means of the PRPD acquisition method.

Key Words: ***electrical insulation, fast switching, overvoltages, partial discharges***

1. INTRODUCTION

Insulating systems of electrical motors in service are subjected to many different stresses. One of the main stresses is the electric field caused by both working voltages and overvoltages. Previously, special attention was paid to voltage distortion manifested by the presence of harmonics. In the last decade the effect of fast rising square voltage waveforms produced by PWM converters (Fig. 1) built on the basis of very fast solid-state switches, e.g. GTO, MOSFET, IGBT type devices started to be treated as even more dangerous [1, 2].

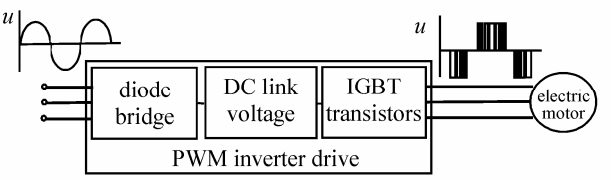

Fig. 1. *The block scheme of motor control with PWM inverter drive*

The pulsed output voltage is applied from PWM drive to the motor terminals by a feeding cable. In those drives the sequence control unit produces pulse-width modulated train of voltage pulses with slew rate up to 100 kV·μs^{-1} and repetition rate up to 100 kHz. (Fig. 2)

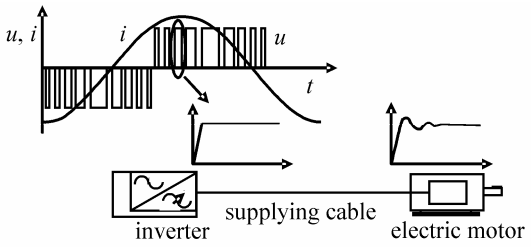

Fig. 2. *Voltage waveforms with overvoltages at converter terminals and supply voltage terminals of an electric motor*

Depending on the rise time of the voltage pulse at the converter output and on the end of the cable, the overvoltage at the motor terminals is generated.

Special problems in the PWM supplied motors, especially with insulation of the first turns of motors windings, arise from electrical stresses generated by:

- pulses with very fast rise times;
- very short times of pulses duration;
- high frequency transient with significant overvoltage;
- influence of cable on magnitude of overvoltages.

Electrical stresses caused by generated supplying voltage distortions often lead to degradation of the insulation systems, their unexpected breakdown and failure of electrical machine. The insulation failure might occur when the magnitude and rise time of the repetitive

transient voltage stress exceeds the withstand capability of the insulating system [3]. The breakdown of insulation will most commonly occur at the highest voltage stress spot, i.e. the first turn of the line end coil to the last turns of the coil group as well as in the endwinding region, where wires from different coils can come into contact.

2. MODELLING OF THE MOTOR-CABLE SYSTEM SUBJECTED TO THE STEP WAVE VOLTAGES

The results of computer modelling of overvoltages stressing insulation system of electrical machines supplied by the PWM inverter-fed drive are presented.

Overvoltages generated at terminals of electric motor supplied by PWM inverter drive were simulated by the use of EMTP-ATP program taking into account parameters of all components of the system.

2.1. Overvoltage parameters

Overvoltages are created by reflected waves at the interface between cable and motor terminals and depend on the converter voltage output, the cable length between the converter and the motor terminals. Due to the non-uniform voltage distribution along the motor winding, the highest magnitude of the overvoltage $U_{\max}$ occurs at the initial turns. Impulse rise time t_r i.e. time for the voltage impulse to go from 0.1 $U_{\max}$ to 0.9 $U_{\max}$ (Fig. 3). The impulse voltage rate $(\mathrm{d}U/\mathrm{d}t)_{\max}$ is described as:

$$\left(\frac{dU}{dt}\right)_{max} = \frac{0.9U_{max} - 0.1U_{max}}{t_r} \qquad (1)$$

The maximum voltage $U_{\max}$ on the winding is equal to $k_{ov}U_a$, where U_a is defined by DC link voltage.

The overvoltage factor k_{ov} depends on the parameters of the supply circuits, including the length of the cable.

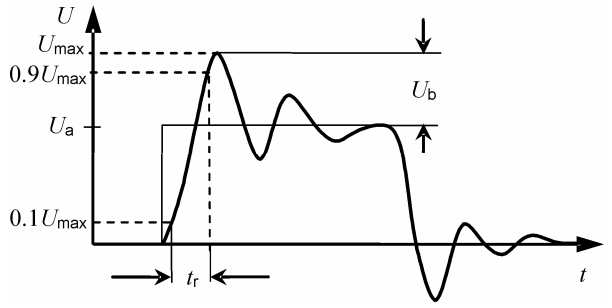

Fig. 3. *Voltage impulse waveshape parameters: U_a - steady state impulse voltage magnitude, U_b - voltage overshoot, t_r - rise time*

2.2. Modelling of motors and cables

Faster, high-current power switching devices give shorter rise times. At each pulse edge, the drive has to charge the capacitance and inductance of the cable, so a pulse of energy is flowing to the cable during each on/off operation.

The length of the cable connecting the drive with electric motor is very important for insulation working conditions in terms of transmission line phenomena leading to arising of internal resonances [2]. There are special rules for proper selection of the cable length and inverter parameters, as the pulses rise time determines the critical cable distance.

The simplified equivalent circuit of motor was used for overvoltages simulations [4-6]. The calculations methodology can be found, e.g. in [4, 7, 8]. Curve 2 in figure 4 shows the frequency dependence of the winding impedance *Z(f)* calculated for parameters of the low voltage 3 kW motor equivalent circuit. The result of wideband impedance measurements for this motor is also shown as a reference (Fig. 4, curve 1) [9, 10].

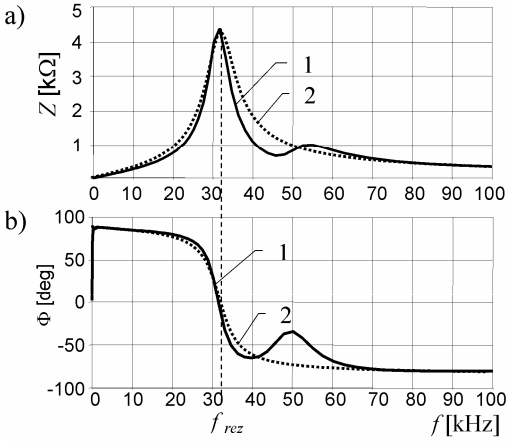

Fig. 4. *Frequency dependence of impedance of one phase of motor winding: a) Z = g(f), b) Φ = g(f) 1 – measured characteristic, 2 – results of simulation*

The pulse propagation velocity in a typical cable is about 170 m/μs. It varies little over the variety of cable types in general use, since it is determined mainly by the permittivity of the internal insulating material.

The supplying cable model can be considered as a long chain of distributed parameters. Frequency dependences of cable parameters should be taken into account. In this paper the model of supply cable was generated with use of procedure *Jmarti_Setup* in EMTP-ATP.

2.3. The modelling of overvoltages on motor terminals

The simulations of overvoltages have been performed in a setup composed of a fast PWM-like generator, cable and a low voltage motor of 3 kW [9]. The IGBT based signal generator is supplying the motor winding with the use of one phase screened cable. The rise time of the switching device is below 0.1 μs.

The results of numerical simulations of overvoltages for supplying cable with different length are presented in figure 5. The maximum value of overvoltages for a system with the supplying cable of 5 m long is equal to 1.4 pu, whereas overvoltages for 85 m length cable reach about 1.6 pu (1 pu refers to the inverter DC link voltage). They confirm the influence of the length of the supplying cables on the maximum value and frequency of overvoltages at the electric machine (Fig. 6). The highest value of overvoltage at the motor is greater for longer cables. The dependence between maximum value of the overvoltage at the motor and the rise time in the range from 0.1 μs to 2 μs for the cables with different length

are presented in figure 7. The simulation results confirm that for shorter rise times of voltage at the PWM inverter output the overvoltages at the motor terminals have higher values.

The visualization of maximum value of overvoltages vs. rise time and the supplying cable length is presented in figure 8.

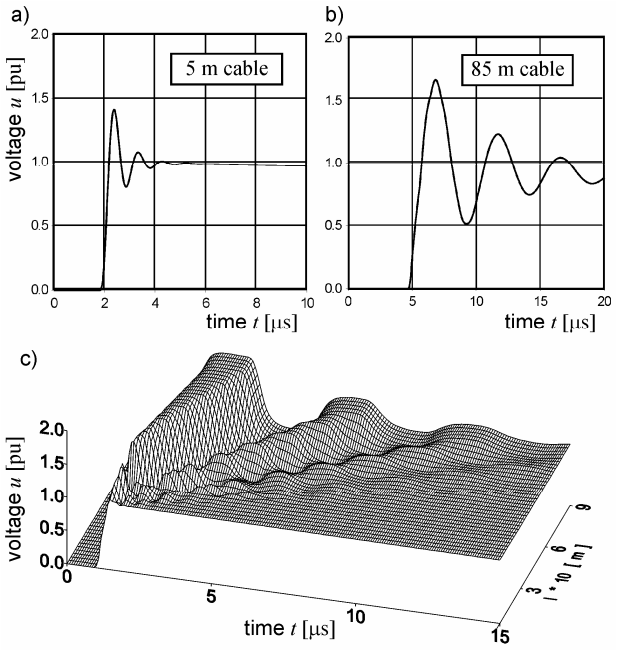

Fig. 5. *Overvoltages at the motor terminals numerically simulated for short (5 m) (a) and long (85 m) (b) supplying cable and 3-D visualization of overvoltages u=f(t, l)(c)*

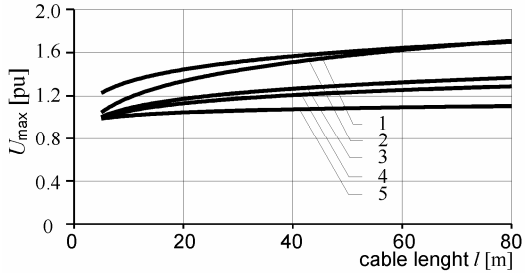

Fig. 6. *Influence of the supplying cable length l on the maximum value of overvoltage U_{max} at motor terminals for t_r: 1) 0.1 μs, 2) 0.25 μs, 3) 0.5 μs, 4) 1 μs, and 5) 2 μs*

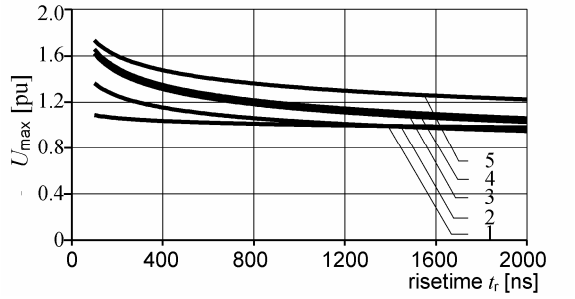

Fig. 7. *The maximum value of overvoltage U_{max} at motor terminals vs. rise time of PWM pulse for different cable length l: 1) 5 m, 2) 10 m, 3) 30 m, 4) 50, and 5) 85 m*

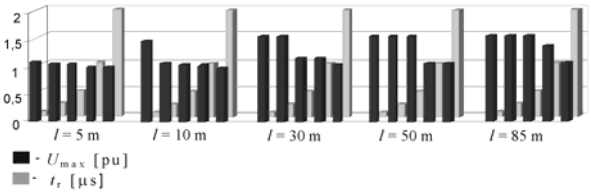

Fig. 8. *The maximum value U_{max} of overvoltage at motor terminals vs. both supplying cable length and rise time of PWM pulse*

3. EXPERIMENTAL RESULTS OF OVERVOLTAGES

The laboratory measurements have been made for a motor supplied by a PWM sequence generator with short (5 m) and long (85 m) feeding cable. Registered overvoltages with an oscillating component are presented in figure 9. The amplitudes of the overvoltages exceed 1.2 pu for short cable and 1.5 pu for long cable.

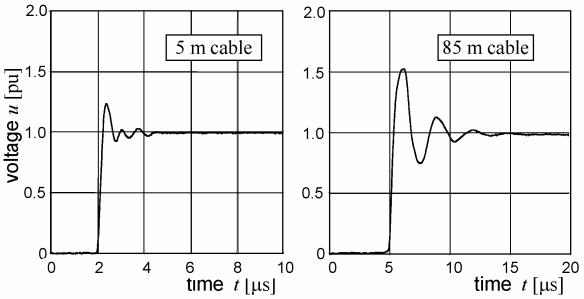

Fig. 9. *Overvoltages recorded at motor terminals for short (5 m) and long (85 m) supplying cable (t_r = 0.5 μs)*

In order to verify the influence of the inverter pulse rise time the measurements have been performed in a configuration, where *cable-motor* system forming transmission *line-load* setup has been energized by voltage pulses with controlled rise time. The rise time has been changed in the range from 100 ns to 10 μs.

The upper traces in figure 10 represent a voltage slope at the inverter output, whereas the lower traces are registered at the motor terminal for a rise time 0.3, 1, 5 and 10 μs, respectively.

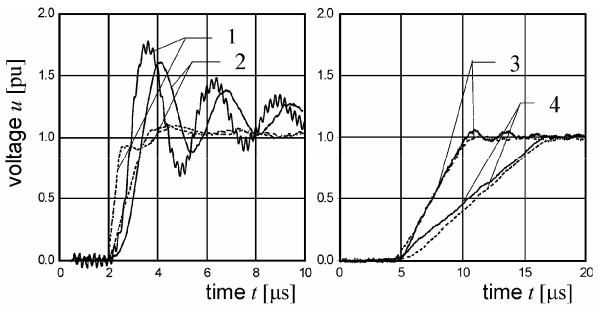

Fig. 10. *Overvoltage at motor terminals (–-) and voltage at inverter output (- - -) for different PWM pulse rise times: 1) 0.3 μs, 2) 1 μs, 3) 5 μs, and 4) 10 μs (cable length l = 85 m)*

The frequency spectrum stimulated by the PWM pulse is closely connected with its slope, then the rise time below 1 μs results in the oscillations generated in

the cable. Simultaneously the overvoltage reaching 1.7 pu for rise time 0.3 μs can be observed. The occurrence of oscillations in a supplying cable treated as a distributed transmission line depends on the relationship between frequency f_{osc} resulting from the cable length and properties determining the speed of the wave propagation, in reference to the spectral content of the pulse dependent on its rise time.

4. MECHANISM OF PARTIAL DISCHARGES AT DIFFERENT VOLTAGE CONDITIONS

4.1. The basic model of PD

In the so-called basic *a-b-c* model of insulating system with PD source the main elements of equivalent circuit are represented by capacitances, e.g. PD source by C_c element (Fig. 11a) [11].

For simulation of real insulating systems supplied from sinusoidal or non-sinusoidal sources also other elements in extended equivalent circuit, e.g. representing volume and surface resistances, should be taken into account. When the insulating system of the electric motor is simulated, both internal and surface discharges should be modeled. In extended equivalent circuits of the motor insulation (Fig. 11b) *n*-parallel branches represent PD sources in defects of insulation. The PD sources are represented by J_1C_1, J_2C_2 elements, and the J_3 represents turn-to-turn surface discharges. These sources can occur in cracks and delaminations formed as a result of degradation processes in insulation.

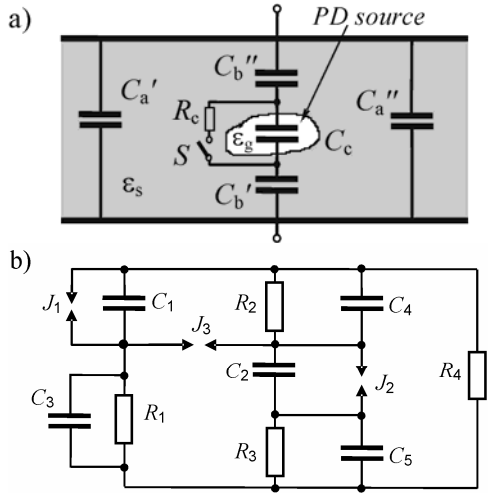

Fig. 11. The equivalent circuit diagrams of electrical insulation with PD sources: a) basic a-b-c model; b) extended scheme of motor insulating system

In the basic model of partial discharge mechanism [12, 13], the constant values of the quantities describing the PD source have been assumed:

– inception voltage U_i,
– extinction voltage U_e,
– charge of PD pulse q_i,
– number of PD pulses in positive and negative half periods of voltage, N^+, and N^-,
– total number of PD pulses N.

The phase range z_φ of discharges in a half cycle of the ac period comprises the angle φ_i, determined by the static inception voltage U_i and the phase angle related to the crest value U_{cm} in the PD source (Fig. 12a) [12].

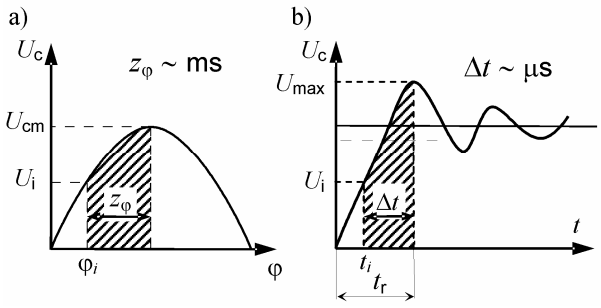

Fig. 12. The phase- or time- range of PD occurrence: a) for sinusoidal voltage (z_φ), and b) for trapezoidal voltage with overvoltage (Δt)

4.2 The model of PD for square voltages

The overvoltage stress may be approximated by trapezoidal shape, with a defined rise time related to the steepness of the trapezoidal slope (Fig. 12b). The rise time t_r depends on a slew rate SR according to:

$$t_r = U_{max} / SR \tag{3}$$

The occurrence of partial discharges depends on the inception voltage U_i in relation to the overvoltages level U_{max}, and can be triggered for $U_{max} > U_i$ (Fig. 12b). The PD intensity and their development are also influenced by the extinction voltage U_e [14]. The time range of PD occurrence is defined by Δt value.

The rise time of the overvoltages depends on the source voltage magnitude and parameters of the motor supply circuits. Assuming the constant values of the voltage U_i and U_e, the voltage drops presented in figures 13a and 13b are equal ($\delta U_1 = \delta U_2$), though the time ranges are different $\Delta t_1 > \Delta t_2$.

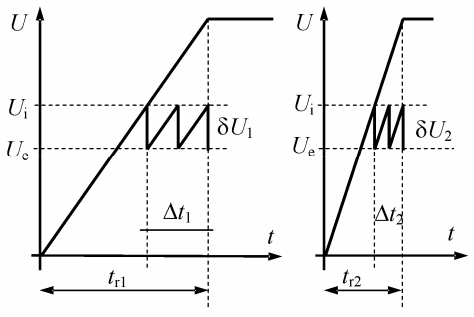

Fig. 13. The PD time range Δt at different rise times $t_{r1} > t_{r2}$

5. RESULTS OF PD MEASUREMENTS

The model of insulating system with a single PD source of epoxy-mica thermosetting insulation has been used in the experiments. The comparison of PD patterns has been performed for:

– sinusoidal waveform 50 Hz,
– square (trapezoidal) voltage waveform 50 Hz with different values of rise times: 3 ms, 1.5 ms, 0.9 ms, and 0.14 ms.

The PD measurements have been made in the system with the HV amplifier controlled by the waveform

generator and the φ-q-n patterns recording system [11, 12]. The PD patterns obtained for trapezoidal waveform (Fig. 14b to 14d) are fundamentally different than PD pattern at sinusoidal voltage (Fig. 14a) and consist of two groups of pulses: first group represents discharges appearing on the rising slope of the trapezoidal voltage whereas the second one corresponds to the flat part of the waveform.

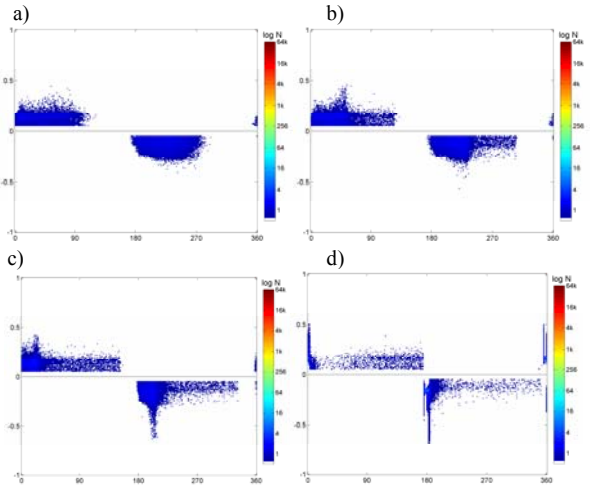

Fig. 14. The PD patterns at: a) sinusoidal voltage, b,c,d,) trapezoidal voltages with rise time t_r: b) 3 ms, c) 1.5 ms, d) 0.14 ms

5. CONCLUSIONS

The electrical motors supplied by modern IGBT based inverters are subjecting the insulation to an additional stress resulting from fast switching; especially fast du/dt slope of the voltage at motor terminals. The supplying cables are also stressed by this process [15].

The frequency response analysis method has been employed to obtain the characteristic frequencies of the cable-motor setup, for both short- and the long-cable supplying system.

Sinusoidal and trapezoidal stimuli have been experimentally compared with respect to PD formation. It was shown that the PD inception voltage could not be predicted from the PD behaviour under ac voltage conditions. It was noticed, that increasing the steepness of the trapezoidal stimulus, the recorded maximum charge magnitude was also increasing. This effect is related to the PD mechanism and may be influenced by the inception delay, which has been observed on PD phase resolved-images in the form of a narrower phase range.

Despite the reduction of the PD occurrence range Δt on rising voltage slope of PWM pulse, the degradation processes could be accelerated by the high repetition rate of the voltage pulses.

ACKNOWLEDGMENT

Researches described in the paper were carried out and used in project no. N R01 0019 04 sponsored by the Polish Ministry of Science and Higher Education

REFERENCES

[1] A.H. Bonnett, *Analysis of the impact of pulse-width modulated inverter voltage wave forms on ac induction motors,* IEEE Annual Pulp & Paper Ind. Techn. Conf., pp. 68-75, 1994

[2] J.A.Oliver, G. C.Stone, *Implications for the applications of adjustable speed drive electronics to motor stator winding insulation,* IEEE El. Insul. Magazine, pp. 32-36, 1995

[3] R.J. Kerkman, D. Leggate, G. Skibinski, *Interaction of drive modulation and cable parameters on AC motor transients,* IEEE Trans. Ind. Appl., vol. 33, No. 3, pp. 722 – 731, 1997

[4] G. Suresh, H.A. Toliyat, D.A. Rendusara, P.N. Enjeti, *Predicting the transient effects of PWM voltage waveform on the stator windings of random wound induction motors*, IEEE Trans. Power Electronics, vol. 14, no. 1, 1999, pp. 23 – 30

[5] M. Kaufhold, H. Auinger, M. Berth, J. Speck, M. Eberhardt, *Electrical stress and failure mechanism of the winding insulation in PWM-inverter-fed LV-motors,* IEEE Trans. Ind. Electron., vol. 47, no. 2, pp. 396-402, 2000

[6] G. Grandi, D. Casadei, A. Massarini, *High frequency lumped parameter model for ac motor windings,* EPE Conf. Proc., 1997, pp. 2.578 - 2.583

[7] J. C. G. Wheeler, *Effects of converter pulses on the electrical insulation in low and medium voltage motors,* IEEE El. Insul. Mag., vol. 21, no. 2, 2005, pp. 22 - 29

[8] A. Boglitteli, A. Cavagnino, M. Lazzari, *Experimental high frequency parameter identification of ac electrical motors*, IEEE on Ind. Appl., vol. 43, no. 1, pp. 5 – 10, Jan./Febr., 2007

[9] B. Florkowska, M. Florkowski, J. Furgał, J. Roehrich, P. Zydroń, *Impact of high frequency switching phenomena on low voltage motor insulation*, Conf. Proc. of INDUCTICA & CWIEME'2009 – Coil Winding, Insulations & Electrical Manufacturing Int. Conf. and Exhibition, Berlin, 2009

[10] M. Florkowski, J. Furgał, *The detection of winding faults in electrical machines using the frequency response analysis method*, Meas. Sci. and Technol., 2004, no. 15, pp. 2067 – 2074

[11] B. Florkowska, M. Florkowski, R. Włodek, P. Zydroń, *Mechanisms, measurements and analysis of partial discharges in diagnostics of high voltage insulating systems*, IPPT PAN, Warszawa, 2001 (written in Polish)

[12] B. Florkowska, *Partial discharges in high voltage insulation systems – analysis of mechanisms, forms and patterns*, IPPT PAN, Warszawa 1997 (written in Polish)

[13] F. H. Kreuger, *Discharge detection in high-voltage equipment,* Butterworth &Co., London, 1989

[14] B. Florkowska, P. Zydroń, *Analysis of conditions of partial discharges inception and development at non-sinusoidal testing voltages*, IEEE CEIDP'2006 Annual Report, October 2006, pp. 648 – 651

[15] S. Grzybowski, P. Shresta, I. Cao, *Electrical aging phenomena of XLPE and EPR cable insulation energized by switching impulses,* Proc. 2008 Int. Conf. on HV Eng. and Appl., Chongqing, China, 2008, pp. 422-425